Int. J. Electrochem. Sci., 8 **(2013)** 578 - 590

International Journal of
ELECTROCHEMICAL
SCIENCE
www.electrochemsci.org

Investigating the Corrosion of API-X100 Pipeline Steel in Aerated Carbonate Solutions by Electrochemical Methods

Faysal Fayez Eliyan[1,*], *El-Sadig Mahdi*[2], *Akram Alfantazi*[1]

[1] Corrosion group, Department of Materials Engineering, The University of British Columbia, Vancouver, BC, Canada, V6T 1Z4
[2] Mechanical Engineering Department, College of Engineering, Qatar University, P.O. Box 2713, Doha, Qatar
*E-mail: faysal09@interchange.ubc.ca

Received: 18 October 2012 / *Accepted:* 29 November 2012 / *Published:* 1 January 2013

This paper explores some key electrochemical aspects associated to the corrosion of API-X100 steel in aerated carbonate solutions. Investigated by polarization and electrochemical impedance spectroscopy tests, the corrosion rates and potentials, the cathodic reactions, and passivation are studied from the perspectives of carbonate content and temperature. The corrosion rates, more sensitive to temperature, were between 12 and 18 μA cm^{-2}, and the corrosion potentials decreased with carbonate content and increased with temperature. And reported for the first time, bicarbonate, which resulted from the CO_3^{2-}/H_2O equilibrium, contributed to the cathodic reactions, and in a manner more significant with carbonate content. The passive films showed evidence that they became more compact with carbonate content, and so with did the lower charge transfer resistance.

Keywords: API-X100, carbonate, polarization, EIS

1. INTRODUCTION

Carbonate is one of the electroactive species that contribute to accelerating and controlling the outer-surface corrosion of the buried pipelines exposed to groundwater, accidently, after coating disbondment, for example [1,2]. Other agents contribute to the dissolution reactions such as bicarbonate, chloride and sulphate, but the effect of carbonate remains, more particularly, chemically and electrochemically pronounced, as it could be sustained in series of aerobic and/or anaerobic reactions before deterioration eventually takes place [3-5]. Carbonate introduced with bicarbonate, in specific, also has long been receiving research interest in relation to studying stress corrosion cracking in high-pH and near-neutral pH solutions. At the crack tip, the propagation is facilitated by dissolution

in the grain boundaries and repeated ruptures of the passive films – whose properties were reported dependent on carbonate [6,7].

This paper aims at exploring the electrochemical role of carbonate in driving the corrosion reactions in aerated solutions. Different from the conventional solutions prepared for SCC tests, no bicarbonate was introduced in order to understand corrosion from narrower chemistry perspectives. If the electrochemical results in this paper are combined with future SCC studies', the already determined role(s) of the environmental factors on the electrochemistry of cracking steels would alleviate the difficulty of analyzing the results. API-X100 is a new pipeline steel of special alloying element content (table 1), and is being considered in some new projects for its high strength, but its corrosion resistance is a new research subject and this paper serves this respect.

The potentiodynamic polarization and other electrochemical techniques were useful in analyzing the corrosion behavior, *i.e*. rates and governing anodic and cathodic reactions, and also the passivation reactions. In an early work by Thomas *et al*. the passivation of pure iron in aerated carbonate solutions at room temperature was studied by stepwise potentiostatic and potentiodynamic polarization techniques [8]. Compared with a $2.5x10^{-3}$ M-hydroxide-potentiodynamic polarization swept with 10 mV min^{-1}, the passivation in the carbonate solutions solely exhibited two characteristic peaks at -0.58 and -0.22 V vs. NHE, which got larger with carbonate concentration. Stikma *et al*. studied the SCC susceptibility and the potentiodynamic behavior of dual-phase and API-X65 steels in 0.5 M $NaHCO_3$ - 0.5 M Na_2CO_3 solutions, which were of a lower pH of 9.5 [9]. With the forward scan of 20 mV min^{-1}, both corrosion and passivation potentials showed a decrease with temperature. But the passivation regime, as well as the findings with the location and size of the anodic peaks, were different from what was reported by Thomas *et al*., and worth being mentioned; the corrosion rates in the two studies were not reported. Performing the potentiodynamic sweeps at lower scan rates was useful in identifying the range of potentials for cracking in carbonate-containing solutions, as reported by Might *et al*. and Parkins *et al.* [10,11]. However, their results did not establish a broad understanding by which the corrosion rates could be predicted, and, in fact, many electrochemical aspects related to passivation and cathodic reactions remained unclear in terms of carbonate. That has also been the case in regard to other physical and chemical factors of carbonate solutions, as well as to other measurement methods and parameters. This research, therefore, attempts to resolve that vagueness in which carbonate is considered the main corrosive agent, and the corrosion behavior is studied with a number of electrochemical methods.

2. EXPERIMENTAL DETAILS

2.1. Corrosion test setup

The experiments were carried out in a standard three-electrode, 1-litre, glass-jacketed cell. The potentials were measured against a saturated calomel electrode of +0.241 V vs. SCE which was kept in a capillary bridge maintained at room temperature. A proper Vycor frit was fitted into the capillary bridge and the counter electrode was a slender graphite rod. The solutions were open to the atmosphere, except that argon was purged for 45 minutes prior to, and throughout the duration of

performing some deoxygenated experiments. A heater circulating a constant-velocity water flow through the cell's jacket to control the test solutions' temperatures at 20, 50 and 90 ^{o}C, was used. A PAR Versastat 4 potentiostat performed the electrochemical experiments, and it was synchronized to VersaStudio software to control the experiments and analyze the results.

2.2. Test material

The API-X100 test coupons were prepared from a pipeline shell manufactured by EVRAZ Inc. The coupons were soldered to thin wires by a conductive paste and mounted in hard epoxy resins that are reliable at high temperatures and in preventing crevice attacks. A sequence of emery papers of 120, 320 and 640-grit were used in getting the samples wet ground. The samples were ultrasonically degreased with ethyl alcohol, rinsed with distilled water, and dried by an air stream. The chemical composition analysis, whose results are summarized in table 1, was carried out by inductive coupled plasma and LECO carbon analysis.

Table 1. Chemical composition of the test material

Composition (wt. %)										C.E.
C	Mn	Mo	Ni	Al	Cu	Ti	Nb	Cr	V	
0.1	1.67	0.21	0.13	0.02	0.25	0.01	0.043	0.016	0.003	0.47

Fig. 1 is a micrograph of the microstructure of an as-received test API-X100 material, obtained from a sample wet-ground up to a 1200-grit emery finish and polished with 6 and 1 μm diamond suspensions. The microstructure consisted of ferrite, pearlite, and bainite with slight microvariations in colour.

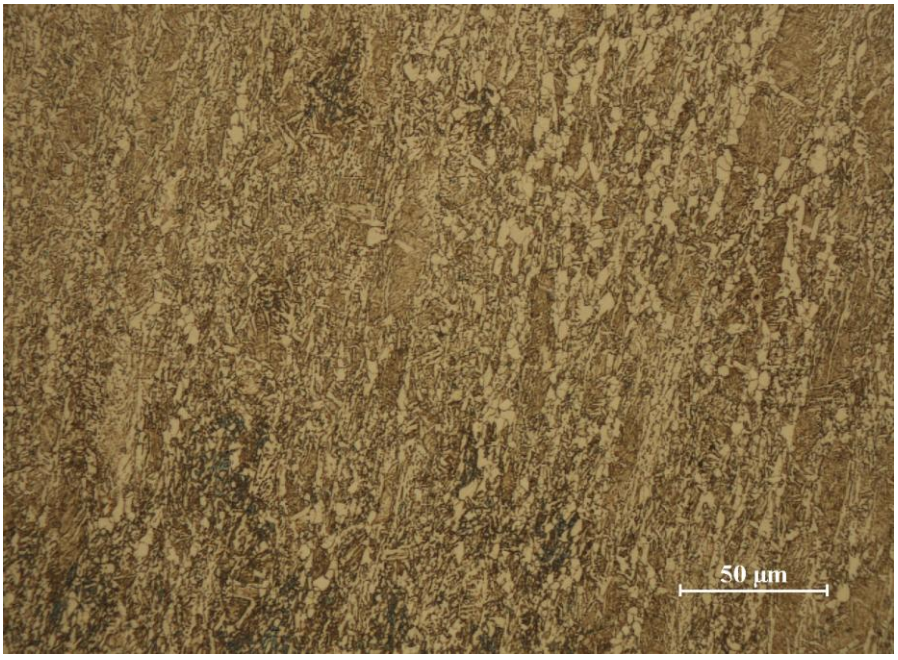

Figure 1. The optical micrograph of API-X100 microstructure.

2.3. Test solutions

The test solutions were synthesized from double-distilled, deionized water, and an analytical grade Fisher procured Na_2CO_3 reagent. The solutions were primarily prepared to be naturally aerated, and contain different concentrations of carbonate of 1, 2, 5, and 10 g L^{-1} at 20, 50, and 90 ^oC. The pH of the solutions was kept unbuffered, in a range between 9.7 and 11.5 in all test solutions. An amount of 100 ppm chloride was introduced to a different batch of solutions, taking into account the same physicochemical factors of the chloride-free solutions.

2.4. Electrochemical tests

The samples, right after immersion in the solutions, were cathodically conditioned at -2 V vs. SCE for 2000 seconds to remove any air-formed oxides. To ensure the reproducibility of the results, the experiments were repeated many times. The potentiodynamic polarization was performed with a forward scan of 0.5 mV sec^{-1} from -1.2 to 1.2 V vs. SCE, and with other scan rates (within the same range) for selected cases. The cathodic polarization behavior was also studied with a scan rate of 0.5 mV sec^{-1}, from -2 V vs. SCE to the corrosion potentials.

The potentiostatic polarization tests were performed at 0 V vs. SCE across a time period of about 3500 seconds, and the EIS tests were performed at the OCPs and 0 V vs. SCE from 10,000 to 0.01 Hz with a sampling rate of 10 points per decade.

3. RESULTS AND DISCUSSION

3.1. Potentiodynamic and potentiostatic polarization tests

Fig. 2 shows the potentiodynamic polarization profiles that describe the corrosion behavior in aerated solutions of different carbonate concentrations and temperatures. The cathodic regimes were generally affected the most by carbonate concentration and so was the passivation at high temperatures. The polarization features were similar to the commonly reported profiles in aerated carbonate/bicarbonate corrosion studies [12,13]. Charge transfer-limited reduction of water was obliterated by the mass transfer-limited reduction of oxygen (Eq. 1) at about -0.97 V vs. SCE. The limiting current density of oxygen reduction in dilute solutions increased from about 50 to 150 μA cm^{-2} at 20, and 50 and 90 ^oC, respectively.

$$O_2 + 2H_2O + 4e^- \rightarrow 4OH^- \qquad E^o = 0.159 \text{ V vs. SCE} \qquad (1)$$

At 20 ^oC, a unique internal cathodic loop appeared in the concentrated solutions at about -0.82 V vs. SCE – a value fairly close to a range of corrosion potentials of steels polarized in aerated bicarbonate solutions [14,15]. This is caused by the reduction of bicarbonate generated from the aqueous equilibrium of carbonate, and its contribution to the reduction reactions seemed dependent on carbonate concentration, which explains the relative increase in the loops' size. Similar loops have

been seldom reported or discussed in association to certain electrochemical aspects. The active anodic regimes were generally similar, and there were small, blunt, anodic peaks that appeared (mostly at 20 ^{o}C) between -0.35 and -0.26 V vs. SCE.

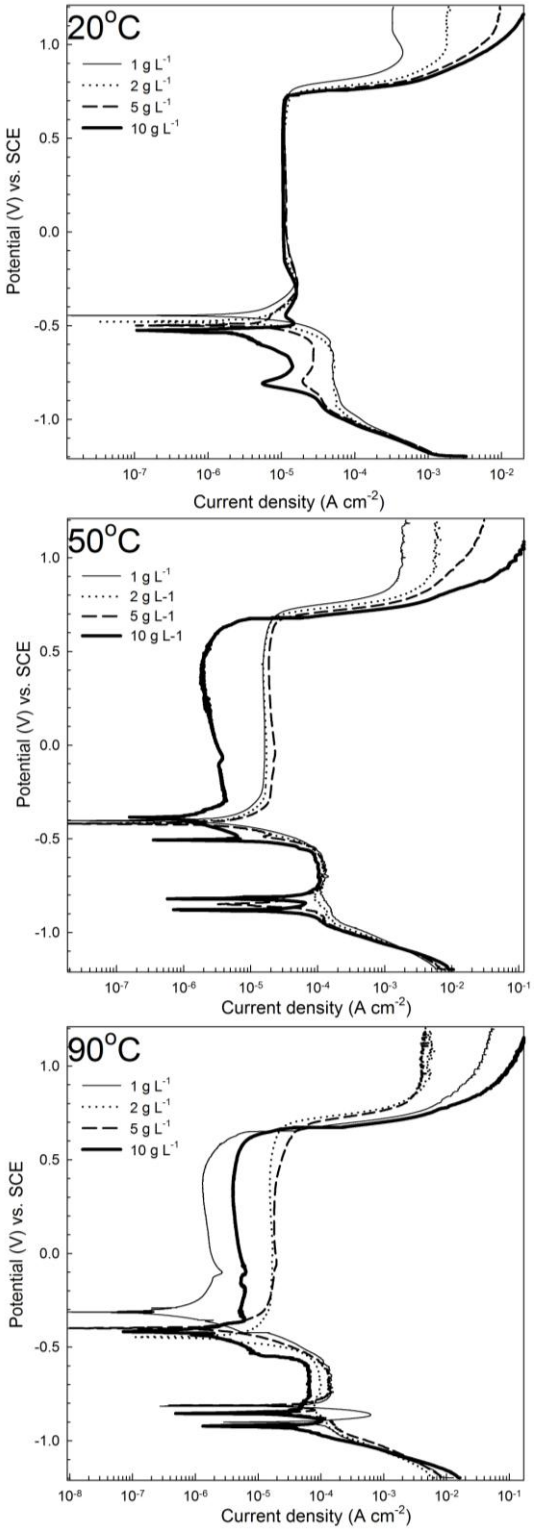

Figure 2. The potentiodynamic polarization in aerated solutions of different carbonate concentrations and temperatures.

The passivation regime was relatively broad and its current was independent from carbonate concentration, which was about 10 μA cm^{-2}, and transpassivation occurred at around 0.7 V vs. SCE. The transpassive currents were proportional with carbonate concentration, and it is interesting to report that peaks appeared at around 0.9 V vs. SCE in the most dilute solutions. At 50 and 90 ^{o}C, the current densities were generally higher and the passivation currents showed a dependence on carbonate concentration.

The passivating films were likely to be comprised primarily from ferrous carbonate and hydroxide, which are highly insoluble in carbonate solutions [16]. In our case, it can be suggested that the passivation formed in two main stages, as $FeCO_3$ initially precipitated as a result of the direct oxidation:

$$Fe + CO_3^{2-} \rightarrow FeCO_3 + 2e^- \qquad E^o = -1 \text{ V vs. SCE} \qquad (2)$$

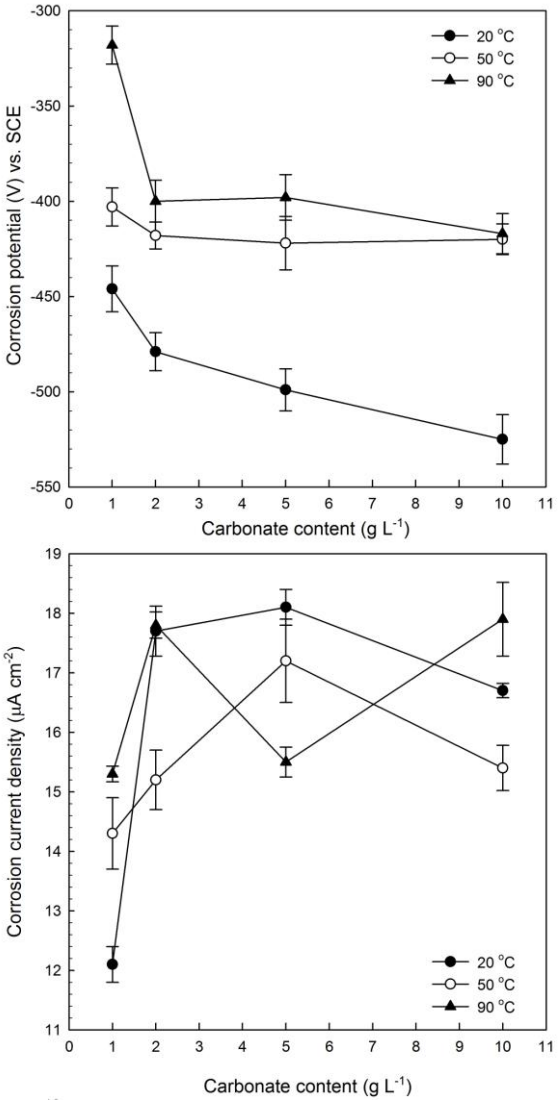

Figure 3. The corrosion potentials and current densities.

The reaction can be well related to the anodic peaks that appeared at around -0.85 V vs. SCE in some dilute and 10 g L^{-1} solutions at high temperatures. As the potentials went more positive, broad peaks appeared – due to oxygen reduction – before the corrosion potentials were reached and other anodic peaks appeared. Some changes in colour were seen during that stage of passivation, suggesting that the passivating films were oxidized. Similar physical and polarization changes were reported by Thomas *et al*. [8] during which the second anodic peak of the passivated iron appeared at -0.22 V vs. NHE (-0.464 V vs. SCE) with a scan rate of 120 mV min^{-1} (2 mV sec^{-1}) in a 0.1 M Na_2CO_3 solution. Depending on a detailed thermodynamic analysis and a previous electron-diffraction examination by Mayne *et al*. [17], Thomas *et al*. reported that γ-Fe_2O_3 forms as a result of $FeCO_3$ oxidation as:

$$2FeCO_3 + 3H_2O \rightarrow Fe_2O_3 + 2CO_3^{2-} + 6H^+ + 2e^- \qquad E^o = -0.764 \text{ V vs. SCE, at pH } 11.3 \qquad (3)$$

The corrosion potentials, as shown in Fig. 3, were less with carbonate concentration and were greater at higher temperature. This suggests an increased anodic sensitivity towards carbonate where the corrosion current densities also showed a slight increase. While there was a discrepancy with the corrosion current densities – being between 12 and 18μA cm^{-2} – with respect to carbonate concentration at a given temperature, the corrosion potentials trend suggests that the cathodic reactions generally decelerates, most probably due to lessened O_2 concentration, in more concentrated carbonate solutions.

The scan rate had an effect on the shape of the polarization profiles, as Fig. 4 shows, especially similar to the passivation reported in [18]. As the scan rate is less, the corrosion potentials were nobler as a result of the deceleration in anodic dissolution. The cathodic reactions, as presented from the mixed charge-mass-controlled reduction of O_2 and H_2O regimes, apparently dominated the behavior during 0.05 and 0.1 mV sec^{-1} polarizations at potentials when the steel underwent dissolution with higher scan rates. The contribution of the charging current density, which proportionally depends on the scan rate and interfacial capacitance [19], was notably very high during 10 and 100 mV sec^{-1} polarizations.

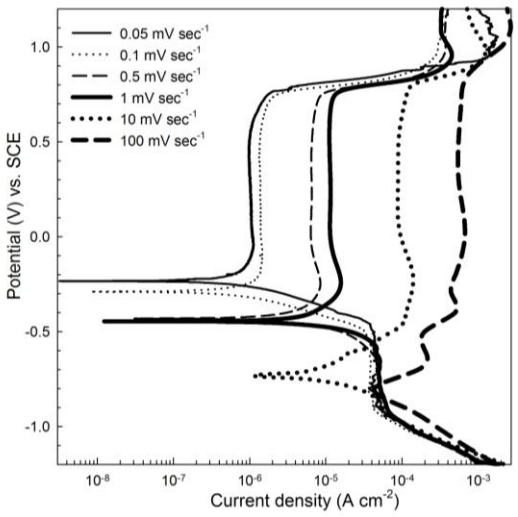

Figure 4. The potentiodynamic polarization carried out with different scan rates in 1 g L^{-1} carbonate solutions at 20 ^oC.

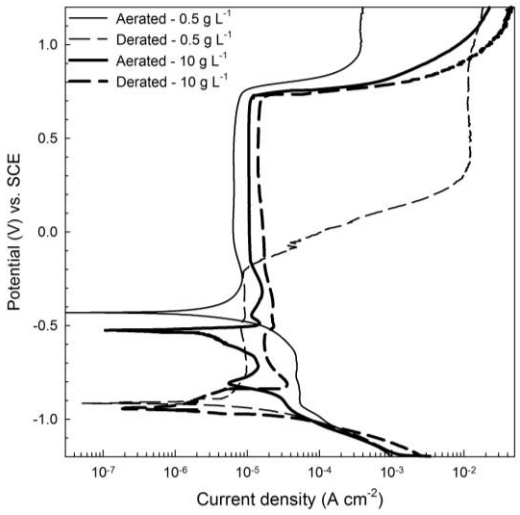

Figure 5. The potentiodynamic polarization in selected aerated and deoxygenated carbonate solutions at 20 ^{o}C.

Fig. 5 shows that, upon deoxygenating the carbonate solutions, the corrosion potentials were notably lower, but the corrosion rates did not show a significant change. Unlike the aerated conditions, the passivation regime appeared broader with carbonate concentration. The cathodic behavior in the aerated 10 g L^{-1} solution suggests that the reduction of O_2 might be sustained, most likely in the concentrated solutions, on early formed $FeCO_3$ above -0.84 V vs. SCE, if compared to the deoxygenated case of the same carbonate content. This however requires a future investigation that takes into account the interfacial physical changes [20]. As Fig. 6 shows, the carbonate content effect was very significant in the mixed charge-mass-transfer-controlled regimes. Above -1 V vs. SCE, the slightly inner cathodic loops in 1 g L^{-1} solutions developed into many peaks in the more concentrated solutions.

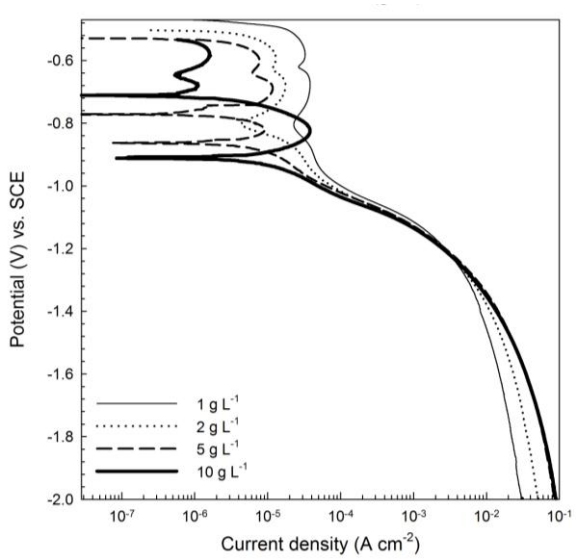

Figure 6. The cathodic polarization at 20 ^{o}C.

The anodic reactions that consume carbonate, bicarbonate and hydroxyl, and as well as the reduction of bicarbonate, which all are reactions that depend on carbonate concentration, contributed to the appearance of these peaks. The limiting current densities showed an increase with carbonate concentration, which were between 30 and 90 mA cm^{-2}, due to a larger role of bicarbonate during the cathodic reactions. An amount of 100 ppm chloride was introduced along with the same factors to study the difference in the polarization behavior from the chloride-free conditions. The polarization profiles (not shown) were not significantly different from the chloride-free conditions, nor were the kinetic parameters. The passivation currents did not exhibit an indication of pitting attack, different from results reported by Deyab *et al*. in bicarbonate/carbonate solutions at 30 ^{o}C, indicating that our 100 ppm chloride is well below the lowest critical 0.1 M concentration considered in that study [21].

The potentiostatic polarization tests were carried out at 0 V vs. SCE – a potential in the potentiodynamic polarization's passivation regime. The variations in the potentiostatic currents usually help provide good clues on the possible physical characteristics/changes in the passive films in relation to the environmental factors.

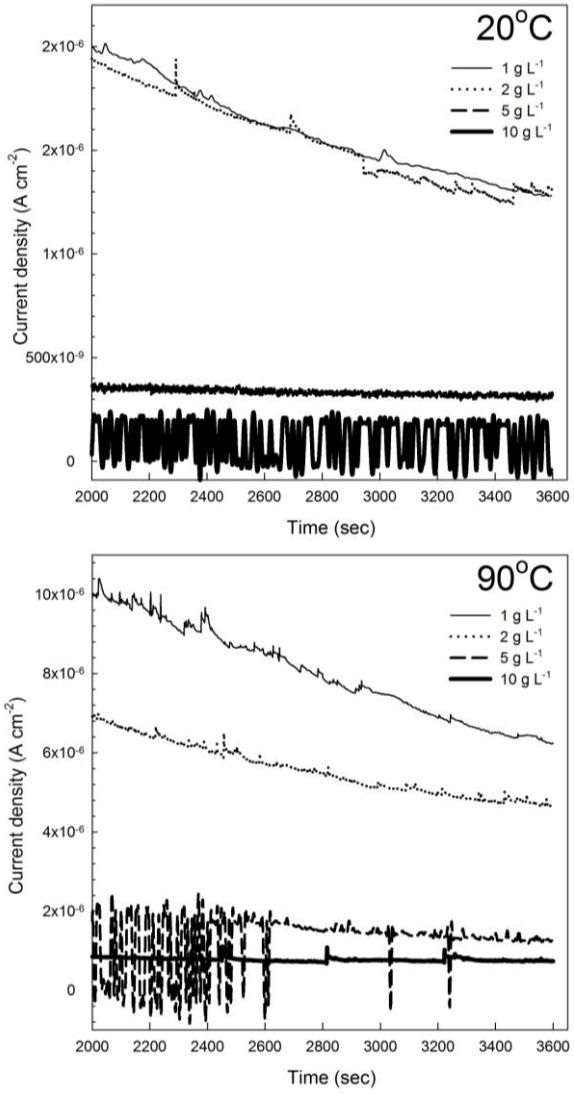

Figure 7. The potentiostatic polarization carried out at 0 V vs. SCE at 20 and 90 ^{o}C.

The profiles shown in Fig. 7 represent the potentiostatic currents at scales in the last 1600 seconds at 20 and 90 ^{o}C. As the currents showed a continuous decay in the dilute solutions of 1 and 2 g L^{-1}, they were largely less and highly stable in 5 and 10 g L^{-1}. This suggests that the passive films were either thicker or more compact in the concentrated solutions, requiring the morphology and composition to be investigated in future studies. The currents were higher at 90 ^{o}C, and there were some fluctuations in the concentrated solutions regardless of temperature, possibly indicating repetitive breakdowns and repassivations [22].

3.2. Electrochemical impedance spectroscopy tests

The EIS tests were carried out to study the possible interfacial processes and the manner they are affected by the environmental factors [23] during the open circuit potential conditions and at 0 V vs. SCE.

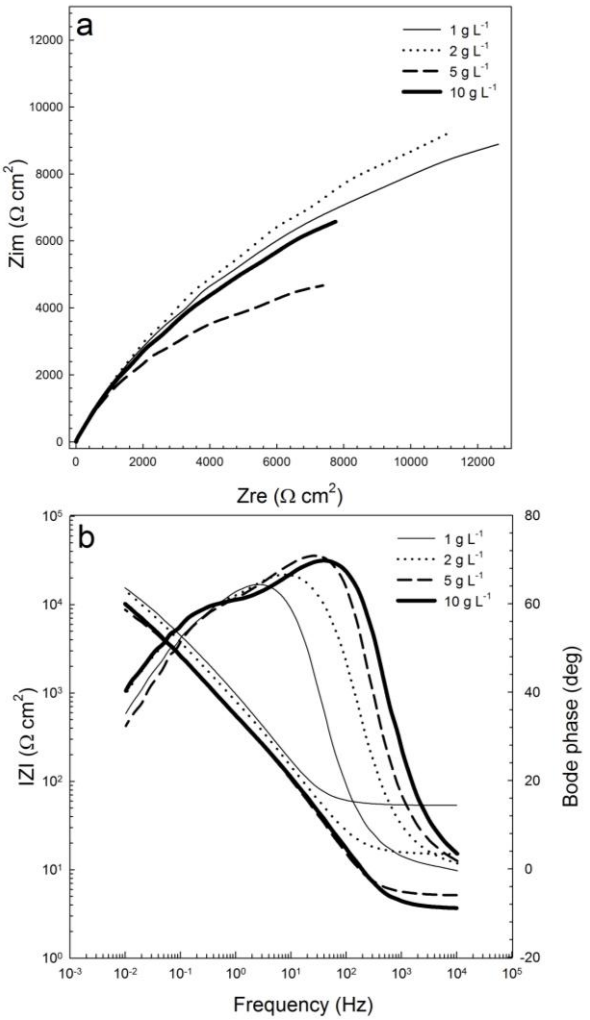

Figure 8. The electrochemical impedance spectroscopy represented by **a** Nyquist, and **b** Bode plots at 20 ^{o}C at the OCPs.

The profiles shown in Figs. 8a and 8b represent the Nyquist and Bode plots of the EIS response as a function of carbonate concentration at 20 ^{o}C at the OCPs. The profiles in general depicted a two-time constant response, and showed that the processes in the double layer – detected across the low-frequency region– were highly affected by electrolyte concentration. The low-frequency capacitive arcs decreased in size, indicating a decrease in charge-transfer resistance in the more concentrated solutions. This agrees with a main finding in the polarization results: higher corrosion rates with higher carbonate content. The solution resistance also largely decreased and the nature of the interactions changed accordingly. They seemed to show a growing change from being relatively governed by adsorption-based interactions to transport-based interactions [24] sustained on/through more compact passive films. That could be related to the shift of the phase peaks to higher frequencies and to the smaller peaks emerging at low frequencies in the concentrated solutions.

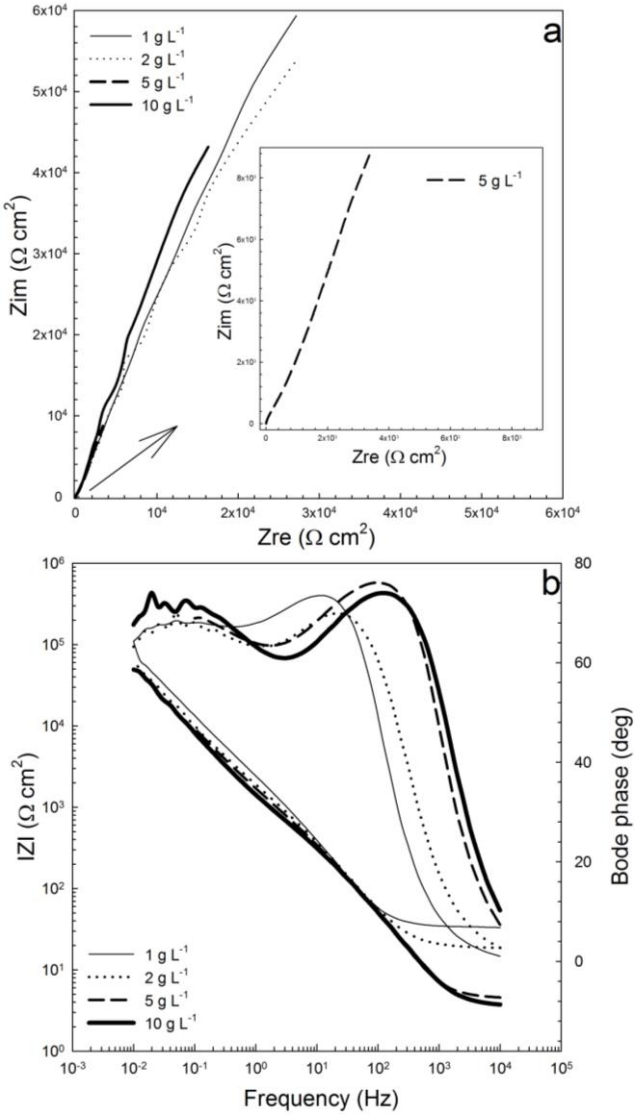

Figure 9. The electrochemical impedance spectroscopy represented by **a** Nyquist, and **b** Bode plots at 20 ^{o}C at 0 V vs. SCE.

At 90 ^{o}C, the Nyquist profiles (not shown) were similar to the 20 ^{o}C conditions', but notably smaller. They also seemed to be primarily governed by adsorption as the high-frequency and low-frequency capacitive arcs were more overlapped. At 0 V vs. SCE, the Nyquist profiles were large and the diffusion tails in all conditions were a predominant feature, as shown in Fig. 9. The response was two-time constant, and the diffusion-limited processes and transport at passivated interfaces governed the interactions. The phase peaks broadening, becoming larger and separated into well-discerned peaks as the solutions were more concentrated, are indicative of effective blocking of the active sites and thickening passivation as a result [25].

4. CONCLUSION

In aerated solutions of different carbonate concentrations and temperatures, the electrochemical corrosion of API-X100 pipeline steel was studied. The potentiodynamic polarization revealed the contribution of oxygen, water, and bicarbonate – an agent naturally exists from carbonate/water equilibrium – into the cathodic reactions. It also revealed evidence of anodic reactions consuming carbonate and hydroxyl in the cathodic regimes, and the dependence of passivation on carbonate content at high temperatures. While the corrosion rates were relatively discrepant, the corrosion potentials decreased with carbonate content and increased with temperature. The potentiostatic currents at 0 V vs. SCE indicated that, regardless of temperature, the passive films become more compact/thicker with increased carbonate content. The EIS response at the OCPs was two-time constant, and showed a decrease in charge-transfer resistance with increased carbonate content and temperature. It was also in agreement, as was with the potentiodynamic polarization behavior, with the main potentiostatic polarization results at 0 V vs. SCE.

ACKNOWLEDGMENT
This publication was made possible by NPRP grant # 09-211-2-089 from the Qatar National Research Fund (a member of Qatar Foundation). The statements made herein are solely the responsibility of the authors.

References

1. J. Beavers, N. Thompson, External corrosion of oil and natural gas pipelines, ASM International, ASM Handbook, Corrosion: Environments and Industries (#05145), 13C, 2006.
2. A.Fu, X. Tang and Y. Cheng, *Corros. Sci*., 51 (2009) 186.
3. C.Lee, Z. Qin, M. Odziemkowski and D. Shoesmith, *Electrochim. Acta*, 51 (2006) 1558.
4. S. Savoye, L. Legrand, G. Sagon, S. Lecomte, A. Chausse, R. Messina and P. Toulhoat, *Corros. Sci.*, 43 (2001) 2049.
5. S. Drissi, Ph. Refait, M. Abdelmoula and J. Génin, *Corros. Sci*., 37 (1995) 2025.
6. B. Fang, A. Atrens, J. Wang, E. Han, Z. Zhu and W. Ke, *J. Mater. Sci*., 38 (2003) 127.
7. R. Parkins and S. Zhou, *Corros. Sci*., 39 (2001) 175.
8. J. Thomas, T. Nurse and R. Walker, *Brit. Corros. J.*, 5 (1970) 87.
9. J. Stikma and S. Bradford, *Corrosion*, 41 (1985) 446.
10. J. Might and D. Duquette, *Corrosion*, 52 (1996) 428.

11. R. Parkins, P. Slattery and B. Poulson, *Corrosion*, 37 (1981) 650.
12. S. Adamy and F. Cala, *Corrosion*, 55 (1999) 825.
13. D. Li, Y. Feng, Z. Bai, J. Zhu and M. Zheng, *Electrochim. Acta*, 52 (2007) 7877.
14. F. Eliyan, E. Mahdi and A. Alfantazi, *Corros. Sci*., 58 (2012) 181.
15. G. Zhang and Y. Cheng, *Electrochim. Acta*, 55 (2009) 316.
16. D. Gilory and J. Mayne, *Brit. Corros. J*., 1 (1966) 161.
17. J. Mayne and J. Menter, *J. Chem. Soc*., (1954) 103.
18. A. Pilkey, S. Lambert and A. Plumtree, *Corrosion*, 51 (1995) 91.
19. A. Bard and L. Faulkner, Electrochemical Methods – Fundamentals and Application, second ed., Wiley, New York, 2001.
20. L. Legrand, S. Savoye, A. Chausse and R. Messina, *Electrochim. Acta*, 46 (2000) 111.
21. M. Deyab and S. Abd El-Rehim, *Electrochim. Acta*, 53 (2007) 1754.
22. Y. Tang and Y. Zuo, *Materials chemistry and physics*, 88 (2004) 221.
23. R. Cottis, S. Turgoose and R. Newman, Corrosion Testing Made Easy: Electrochemical Impedance and Noise, NACE International, USA, 1999.
24. D. Li, Y. Feng, Z. Bai, J. Zhu and M. Zheng, *Electrochim. Acta*, 52 (2007) 7877.
25. F. Farelas, M. Galicia, B. Brown, S. Nesic and H. Castaneda, *Corros. Sci.*, 52 (2010) 509.